Redox Biology 66 (2023) 102850

Contents lists available at ScienceDirect

Redox Biology

journal homepage: www.elsevier.com/locate/redox

Gene deletion of long-chain acyl-CoA synthetase 4 attenuates xenobiotic chemical-induced lung injury via the suppression of lipid peroxidation

Yuki Tomitsuka [a], Hiroki Imaeda [a], Haruka Ito [a], Isaki Asou [a], Masayuki Ohbayashi [b], Fumihiro Ishikawa [c], Hiroshi Kuwata [a], Shuntaro Hara [a,*]

[a] Division of Health Chemistry, Department of Healthcare and Regulatory Sciences, School of Pharmacy, Showa University, 1-5-8 Hatanodai, Shinagawa-ku, Tokyo, 142-8555, Japan

[b] Division of Pharmacotherapeutics, Department of Clinical Pharmacy, School of Pharmacy, Showa University, 1-5-8 Hatanodai, Shinagawa-ku, Tokyo, 142-8555, Japan

[c] Center for Biotechnology, Showa University, 1-5-8 Hatanodai, Shinagawa-ku, Tokyo, 142-8555, Japan

ARTICLE INFO

Keywords:
Long-chain acyl-CoA synthetase 4
ACSL4
Paraquat
Methotrexate
Lipid peroxide
Ferroptosis

ABSTRACT

Long-chain acyl-CoA synthetase (ACSL) 4 converts polyunsaturated fatty acids (PUFAs) into their acyl-CoAs and plays an important role in maintaining PUFA-containing membrane phospholipids. Here we demonstrated decreases in various kinds of PUFA-containing phospholipid species in ACSL4-deficient murine lung. We then examined the effects of ACSL4 gene deletion on lung injury by treating mice with two pulmonary toxic chemicals: paraquat (PQ) and methotrexate (MTX). The results showed that ACSL4 deficiency attenuated PQ-induced acute lung lesion and decreased mortality. PQ-induced lung inflammation and neutrophil migration were also suppressed in ACSL4-deficient mice. PQ administration increased the levels of phospholipid hydroperoxides in the lung, but ACSL4 gene deletion suppressed their increment. We further found that ACSL4 deficiency attenuated MTX-induced pulmonary fibrosis. These results suggested that ACSL4 gene deletion might confer protection against pulmonary toxic chemical-induced lung injury by reducing PUFA-containing membrane phospholipids, leading to the suppression of lipid peroxidation. Inhibition of ACSL4 may be promising for the prevention and treatment of chemical-induced lung injury.

1. Introduction

Pulmonary tissue can be damaged in different ways, such as by inflammation, ischemia–reperfusion, or exposure to either mineral dust or normobaric pure oxygen levels. Pulmonary tissue is also damaged by a variety of xenobiotic chemicals, such as paraquat (PQ) and methotrexate (MTX). It has been reported that reactive oxygen species (ROS), which such chemicals can generate through various pathways, are partly responsible for such damage [1,2]. PQ, a pesticide, is highly toxic to the lungs and has a high mortality rate [1,3]. PQ is selectively taken up into the lungs by the polyamine transporter. Inside the lungs, PQ is transformed into PQ radicals [4]. These radicals then undergo a Fenton reaction, resulting in the production of ROS, including hydroxy radicals [5], which damage pulmonary tissue. MTX is used as both a rheumatoid arthritis (RA) therapeutic and an anticancer drug [6], but long-term use of MTX to treat RA patients often results in side effects such as pulmonary fibrosis [7–9]. MTX increases ROS levels in lung tissue, and the involvement of ROS production in MTX-induced pulmonary fibrosis has been also indicated [10,11]. However, the precise mechanism by which chemical-induced ROS generation leads to pulmonary damage has not been fully elucidated.

ROS can react with the polyunsaturated fatty acids (PUFAs) of membrane phospholipids and induce lipid peroxidation. Lipid peroxides induce cellular/subcellular membrane damage and interact with proteins and DNA, leading to cell death [12,13]. Thus, PUFA-containing membrane phospholipids are potential targets for ROS, and their cellular levels might be correlated with sensitivity to ROS-induced cell death. The levels of PUFA-containing phospholipids are maintained by phospholipid remodeling reactions. Long-chain acyl-CoA synthetases (ACSLs), which convert long-chain fatty acids into their acyl-CoAs, play an important role in phospholipid remodeling. Currently, five ACSL isozymes have been identified in mammals: ACSL1, ACSL3, ACSL4, ACSL5, and ACSL6 [14]. Among these, ACSL4 prefers polyunsaturated fatty acids (PUFAs) such as arachidonic acid (AA), eicosapentaenoic acid (EPA), docosahexaenoic acid, and adrenic acid. ACSL4 plays a crucial

* Corresponding author.
E-mail address: haras@pharm.showa-u.ac.jp (S. Hara).

https://doi.org/10.1016/j.redox.2023.102850
Received 30 June 2023; Received in revised form 10 August 2023; Accepted 11 August 2023
Available online 12 August 2023

Abbreviations

AA	arachidonic acid
ACSL	long-chain acyl-CoA synthetase
BALF	bronchoalveolar lavage fluid
BMDM	bone marrow-derived macrophage
COX-2	cyclooxygenase-2
DPPC	dipalmitoyl PC
EPA	eicosapentaenoic acid
ESI-MS	electrospray ionization mass spectrometry
FCS	fetal calf serum
Fer-1	ferrostatin-1
GPx4	glutathione peroxidase 4
HE	Hematoxylin-Eosin
KO	knockout
LC	liquid chromatography
LPCAT	lysophosphatidylcholine acyltransferase
Micro-CT	micro-computed tomography
MS	mass spectrometry
MTX	methotrexate
PBS	phosphate buffered saline
PC	phosphatidylcholine
PE	phosphatidylethanolamine
PQ	paraquat
PUFA	polyunsaturated fatty acid
qRT-PCR	real-time quantitative RT-PCR
RA	rheumatoid arthritis
ROS	reactive oxygen species
TBS	Tris-buffered saline
WT	wild-type

role in maintaining phospholipids containing PUFAs within the body [15–18]. We found lower levels of PUFA-derived fatty acyl-CoA and PUFA-containing phospholipids in bone marrow-derived macrophages (BMDMs) obtained from ACSL4-deficient mice compared to those of wild-type (WT) mice [18]. Recently, ferroptosis (iron-dependent cell death) was identified as a new form of regulated cell death [19], which is caused by the accumulation of lipid peroxides derived from PUFA-containing phospholipids [19,20]. It has been shown that deletion of ACSL4 suppresses ferroptosis [21–23], while deletion of glutathione peroxidase 4 (GPx4), which eliminates phospholipid peroxides, promotes ferroptosis [24]. We recently found ACSL4 deletion prevented acetaminophen-induced acute liver failure [25]. These findings suggest that ACSL4 may be involved in ROS-mediated cell death and tissue injury via the incorporation of PUFAs into membrane phospholipid. However, the involvement of ACSL4 in xenobiotic chemical-induced pulmonary toxicity is still unclear.

In this study, we investigated the impact of ACSL4 deficiency on phospholipid species containing PUFA in murine lungs. We observed decreased levels of various types of these phospholipid species in ACSL4-deficient lungs. We then examined the effects of ACSL4 deficiency on lung injury induced by PQ and MTX. The results showed that ACSL4 deficiency mitigates both PQ- and MTX-induced lung injury by suppressing lipid peroxidation.

2. Materials and methods

2.1. Materials

PQ dichloride (1,1-dimethyl-4,4-dipyridinium dichloride) and MTX were purchased from FUJIFILM Wako Pure Chemical Corporation (Osaka, Japan). Rabbit antibodies against ACSL4 (FACL4: ab155282) were purchased from Abcam (Cambridge, MA, USA). Mouse monoclonal antibodies against β-actin were purchased from Sigma Aldrich (St. Louis, MO, USA). Rat monoclonal antibodies against mouse Ly6G (clone 1A8) were purchased from Bio X cell (Lebanon, NH, USA). The DAKO Envision^{+} system peroxidase kit was purchased from DAKO (Carpinteria, CA, USA). Anti-mouse CD11b-FITC (11-0112-82), anti-mouse Ly-6G/6C-PE (12-5931-82), and anti-mouse F4/80-PE-Cy5 (15-4801-82) antibodies were purchased from eBioscience (San Diego, CA, USA). Ferrostatin-1 (Fer-1) was purchased from Cayman Chemical (Ann Arbor, MI, USA).

2.2. Animals

Male 7- to 12-week-old Balb/c mice were used. Disrupted murine ACSL4 locus and knockout (KO) mice carrying the Acsl4t$^{m1a(EUCOMM)Wtsi}$ allele (EM:05887) were generated by the European Conditional Mouse Mutagenesis Program (EUCOMM) consortium. Female ACSL4 heterozygous KO mice (ACSL4$^{+/-}$) were obtained from the European Mouse Mutant Archive and then back-crossed with Balb/c mice. Male ACSL4 KO mice (ACSL4$^{-/Y}$: ACSL4 KO) were generated by interbreeding male ACSL4 WT (ACSL4$^{+/Y}$: ACSL4 WT) mice with female ACSL4$^{+/-}$ heterozygous KO mice. All animal experimental procedures were approved by the Institutional Animal Care and Use Committees of Showa University.

2.3. PQ- and MTX-induced lung injury

PQ was dissolved in saline and administered intraperitoneally to WT or ACSL4 KO mice at a single dose of 25 mg/kg body weight. For pretreatment with Fer-1, mice were administered Fer-1 (0.8 mg/kg) via tail vein injection 1 h before PQ administration and then Fer-1 was administered once a day beginning the next day. Mice were monitored once daily for survival for up to 28 days. For histological or gene expression analysis, the lungs were collected 3 days after injection of PQ.

MTX was dissolved in saline and administered orally at a single dose of 3 mg/kg body weight daily for 21 consecutive days as described previously [26]. For pretreatment with Fer-1, mice were administered Fer-1 (0.8 mg/kg) via tail vein injection 1 h before MTX administration every day. Mice were sacrificed on day 21 after daily administration of MTX, and the lungs were fixed with 4% paraformaldehyde or snap-frozen in liquid nitrogen.

2.4. Preparation of lung tissue homogenates, bronchoalveolar lavage fluid (BALF), and cells

The lungs were homogenized in 500 μL of SET buffer (250 mM sucrose, 1 mM EDTA, 10 mM Tris-HCl; pH 6.8) followed by centrifugation at 10,000×*g* at 4 °C for 5 min. After centrifugation, protein concentrations were quantified using the Pierce BCA protein assay kit (Thermo Scientific, Waltham, MA, USA) according to the manufacturer's instructions. Bronchoalveolar lavage was performed by cannulating the trachea with a 27-gauge indwelling needle and infusing it three times with 1 mL of phosphate-buffered saline (PBS) containing 2% fetal calf serum (FCS). After centrifugation, BALF and cells were collected.

2.5. Electrospray ionization mass spectrometry (ESI-MS) analysis

All mass spectrometric analyses were performed using the Prominence HPLC system (Shimadzu, Kyoto, Japan) equipped with a linear ion trap quadrupole mass spectrometer (QTRAP5500 or QTRAP6500, Sciex, Framingham, MA, USA). Phospholipids were quantified using the liquid chromatography (LC)-QTRAP5500 MS/MS via multiple-reaction monitoring in negative-ion mode as previously reported [16]. Fatty

acyl-CoA species were quantified using the LC-QTRAP6500 MS/MS as previously reported [18]. For the quantification of oxidized phospholipid species, a 10 μL sample was injected into an XBridge BEH C18 column (150 × 1.0 mm inner diameter, 3.5 μm particle, Waters, Milford, MA, USA) in LC equipped with QTRAP5500. Solvent A consisted of 0.1% formic acids and 0.028% ammonia in acetonitrile/methanol/water (2:2:1, v/v), and solvent B consisted of 0.1% formic acid and 0.028% ammonia in isopropanol. The gradient conditions were A: B = 100:0 (0–5 min), 50:50 (5–25 min), 50:50 (25–59 min), 100:0 (59–60 min), and 100:0 (60–75 min) at a flow rate of 70 μL/min. Detection was performed in negative ion mode with the following settings: ion spry voltage, −4500 V; collision gas (N_2), 'medium'; declustering potential, −60 V; collision energy, −40 eV; temperature, 300 °C.

2.6. Western blotting analysis

Lung tissues were homogenized in SET buffer, and the protein concentrations were measured using the BCA protein assay kit (Thermo Fisher Scientific, Waltham, MA, USA). These protein samples were subjected to SDS-PAGE using 10% (w/v) gels, transferred to nitrocellulose membranes (GE Healthcare Sciences, Marlborough, MA, USA) with a bath-type blotter. After blocking for 0.5 h, membranes were incubated with anti-ACSL4 (1:5000) or anti-β-actin (1:10,000) antibodies at 4 °C overnight. The membranes were then incubated with horseradish peroxidase-conjugated anti-mouse (1:3000 for β-actin) or anti-rabbit (1:3000 for ACSL4) IgGs, and the blots were visualized using Western Lightning Chemiluminescence Reagent Plus (PerkinElmer Life Sciences, Wellesley, MA, USA).

2.7. Histological analysis

The extracted lungs were fixed in 4% paraformaldehyde and embedded into paraffin, then were cut into 5-μm-thick sections. Hematoxylin-eosin (HE) staining was performed with hematoxylin for 5 min and eosin for 5 min. Masson's trichrome staining was performed using the standard Masson's trichrome stain kit protocol (HT15, Sigma Aldrich).

For immunohistochemistry, antigen retrieval was performed by 10 mmol/L of Tris-HCl (pH 8.8) buffer. Following the inhibition of endogenous peroxidase using 3% H_2O_2 in Tris-buffered saline (TBS), the sections were incubated overnight at 4 °C with a rabbit monoclonal anti-ACSL4 antibody and a rat monoclonal anti-Ly6G antibody (1:3000, 1:500 dilution each). The sections were washed three times with TBS, and then the corresponding secondary antibodies were applied and incubated for 1 h at room temperature. Immunohistochemistry was performed using a Dako EnVision + System with an HRP-labeled polymer anti-rabbit antibody (DAKO, Carpinteria, CA, USA) according to the manufacturer's instructions and then counterstained with hematoxylin. The image was captured with a microscope (BZ-X810; Keyence, Osaka, Japan).

2.8. RT-PCR analysis

Total RNA was extracted from the lung tissues using TRIzol reagent (Invitrogen, Carlsbad, CA, USA) according to the manufacturer's instructions. The total RNA was reverse-transcribed into cDNA using the High-Capacity cDNA Reverse Transcription Kit (Applied Biosystems, Foster City, Waltham, MA, USA) according to the manufacturer's protocol.

Real-time quantitative RT-PCR (qRT-PCR) was performed on a Step One Plus real-time PCR system (Applied Biosystems). Each sample was individually loaded into a 10 μL reaction using SYBR Green PCR Master Mix (Applied Biosystems). PCR cycling conditions included an initial cycle of denaturation at 95 °C for 10 min, followed by 40 cycles of denaturation at 95 °C for 3 s and annealing/extension at 60 °C for 45 s. Dissociation curves were collected to verify the specificity of the PCR, and standard curves were generated using 1:4 serial dilutions of the template cDNA. Gene expression was quantified using the standard curve and normalized to 18S ribosomal RNA. The following primers were used: 18S ribosomal RNA, Forward: 5′-TTCGTATTGCGCCGCTAGA-3'; Reverse: 5′-CTTTCGCTCTGGTCCGTCTT-3'. IL-6, Forward: 5′-GAGGATACCACTCCCAACAGACC-3'; Reverse: 5′-AAGTGCATCATCGTTGTTCATACA-3'. IL-1β, Forward: 5′-GCAACTGTTCCTGAACTCAACT-3'; Reverse: 5′-ATCTTTTGGGGTCCGTCAACT-3'. CXCL1, Forward: 5′-GCAGACCATGGCTGGGATT-3'; Reverse: 5′-CCTGAGGGCAACACCTTCAA-3'. CXCL2, Forward: 5′-GCGCCCAGACAGAAGTCATAG-3'; Reverse: 5′-AGGGTCAAGGCAAACTTTTTGA-3'. CXCL5, Forward: 5′-CGGTTCCATCTCGCCATTCA-3'; Reverse: 5′-GCTATGACTGAGGAAGGGGC-3'. CXCR2, Forward: 5′-TGCTACTAGCCTGCATCAGC-3'; Reverse: 5′-ATGGGCAGGGCCAGAATTAC-3'. COX-2, Forward: 5′-CAGCCAGGCAGCAAATCC-3'; Reverse: 5′-ACATTCCCCACGGTTTTGAC-3'. ACSL4, Forward: 5′-CCAAAGAACACCATTGCCATT-3'; Reverse: 5′-AAGTCTGTGCTGCAATCATCCA-3'. GPx4, Forward: 5′-GCCAAAGTCCTAGGAAACGC-3'; Reverse: 5′-CCGGGTTGAAAGGTTCAGGA-3'.

2.9. Micro-computed tomography (micro-CT) analysis

Lungs were analyzed the third day after injection of PQ using micro-CT systems (R_mCT2; Rigaku, Tokyo, Japan). Mice were anesthetized with 3% isoflurane (Dainippon Sumitomo Pharmaceutical Co. Ltd., Osaka, Japan) and scanned for 4.5 min with a resolving power of 93 μm, 512 slices, 90 kV tube voltage, and 160 μA tube current. 2D images of the 512 slices obtained from micro-CT were converted to 3D image segmentations of lungs and airways, and then analyzed by Analyze 11.0 software (Analyze Direct; Overland Park, KS, USA) in accordance with the manufacturer's instructions.

2.10. Flow cytometric analysis

Flow cytometric analysis was performed on BALF cells. Cells were suspended in RBC lysis buffer (17 mM Tris-HCl, 0.75% NH_4Cl) and allowed to stand for 5 min at room temperature. After 10% FCS DMEM was added to stop the reaction, cells were centrifuged and washed in 10% FCS DMEM. After resuspension in 2% FCS PBS (−), cells were stained with either anti-CD11b-FITC, anti-Ly-6G/6C-PE, or anti-F4/80-PE-Cy5 antibody. The stained cells were analyzed with MoFlo Astrios EQ (Beckman Coulter, Fullerton, CA, USA) using Kaluza Analysis Software 2.1 (Beckman Coulter).

2.11. Hydroxyproline assay

Lungs of MTX-treated mice were cut into small pieces and homogenized in 1 mL of 0.5 M acetic acid containing 1 mg pepsin and mixed overnight at room temperature. Collagen content was measured using the Sircol Soluble Collagen Assay (Biocolor, Newtownabbey, Northern Ireland) according to the manufacturer's instructions.

2.12. Statistical analysis

Data were expressed as means ± SEM. Statistical comparisons between two groups were conducted using the Student's unpaired two-tailed *t*-test, while comparisons among three or more groups were performed using two-way analysis of variance (ANOVA) followed by the Tukey-Kramer post-hoc test. The survival curve was plotted using the Kaplan-Meier method and compared with the generalized Wilcoxon test. A *P* value less than 0.05 was considered statistically significant. All statistical analysis was performed using JMP pro version 16 (SAS Institute Inc., Cary, NC, USA).

3. Results

3.1. Effect of ACSL4 deficiency on phospholipid composition in lung

As shown in Fig. 1A, ACSL4 protein was expressed in lungs from WT mice, whereas the expression of ACSL4 protein in KO mice was reduced dramatically, to undetectable levels, in Western blotting. We previously reported that the levels of PUFA-derived fatty acyl-CoA and those of PUFA-containing phospholipids were lower in ACSL4-deficient BMDMs than in WT BMDMs. Thus, in this study we first investigated the long-chain acyl-CoA levels in mouse lung by LC-MS/MS. This revealed that, as was the case in BMDMs, the levels of acyl-CoA derived from AA (C20:4) and EPA (C20:5), both of which have been reported to be good substrates for ACSL4, were significantly reduced in lungs by the gene deletion of ACSL4 (Fig. 1B). In contrast to these acyl-CoAs, no differences between the two genotypes were observed in the levels of saturated and monounsaturated fatty acyl-CoAs, or in the levels of C18:2-CoA and C18:3-CoA in lungs.

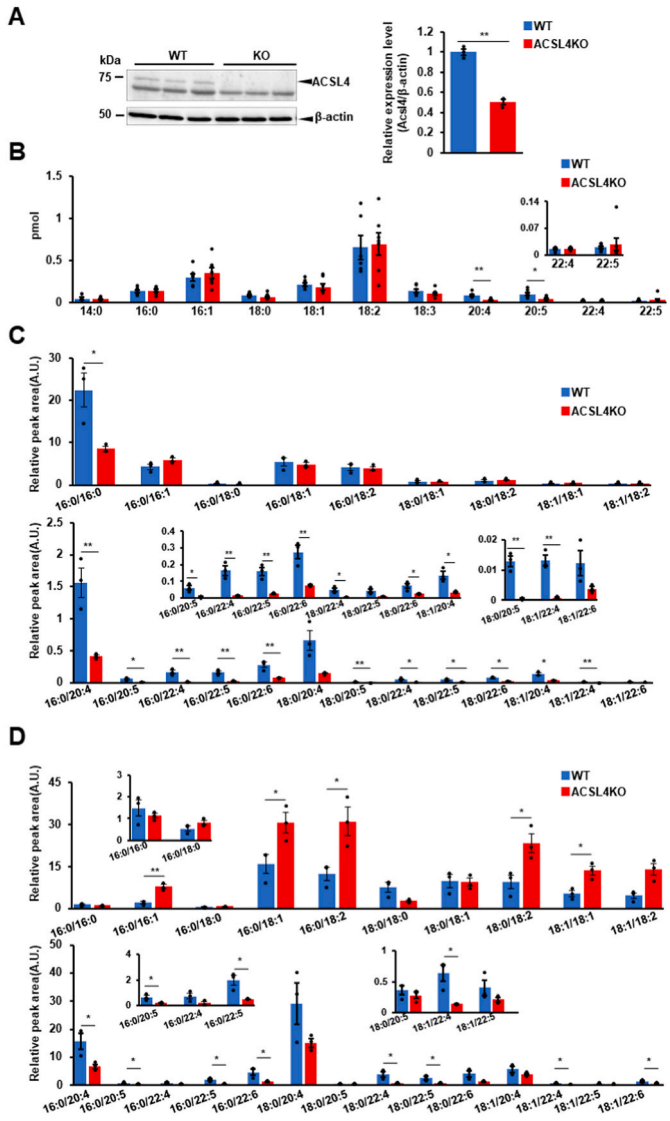

Fig. 1. Effects of ACSL4 deficiency on the levels of fatty acyl-CoA content and membrane phospholipid composition in mouse lung tissues. (A) Expression of ACSL4 proteins in lung tissues of WT and ACSL4 KO mice. Lung tissue homogenates of WT or ACSL4 KO mice were subjected to Western blotting and densitometric quantification of ACSL4; n = 3/group. **(B)** LC-MS/MS quantitation of fatty acyl-CoA content in lung tissues of WT (blue columns) and ACSL4 KO mice (red columns); n = 6–7/group. **(C)** Fatty acid composition of PC species in lung tissues of WT and ACSL4 KO mice. PC species bearing only saturated, monounsaturated, or divalent unsaturated fatty acids (upper) and PUFAs (lower) in lung tissues of WT (blue columns) and ACSL4 KO mice (red columns); n = 3/group. **(D)** Fatty acid composition of PE species in lung tissues of WT and ACSL4 KO mice. PE species bearing only saturated, monounsaturated, or divalent unsaturated fatty acids (upper) and PUFAs (lower) in lung tissues of WT (blue columns) and ACSL4 KO mice (red columns); n = 3/group. Data represent means ± SEM. $*p < 0.05$ and $**p < 0.01$, WT vs ACSL4 KO mice. (For interpretation of the references to color in this figure legend, the reader is referred to the Web version of this article.)

We further examined the effects of ACSL4 deletion on the acyl-chain composition of phospholipids in lungs. Our LC-MS/MS analysis revealed that the knockout of ACSL4 decreased the levels of phosphatidylcholines (PCs) and phosphatidylethanolamines (PEs), which contain AA, EPA, adrenic acid (C22:4), and docosapentaenoic acid (C22:5) at the *sn*-2 position (Fig. 1C and D). The levels of AA-containing phosphatidylglycerol and EPA-containing phosphatidylinositol were also lower in KO mice than in WT mice (Suppl. Fig. 1). On the other hand, PE with palmitic acid (C16:0), palmitoleic acid (C16:1), stearic acid (C18:0), oleic acid (C18:1), and linoleic acid (C18:2) were found at higher levels in KO mice than in WT mice. Phosphatidylserine with palmitic acid (C16:0), oleic acid (C18:1), and linoleic acid (C18:2) was also increased in KO mice (Suppl. Fig. 1).

Interestingly, dipalmitoyl PC (DPPC, 16:0–16:0 PC), a major component of pulmonary surfactant [27,28], was lower in KO murine lungs than in WT mouse lungs. However, the expression level of lysophosphatidylcholine acyltransferase (LPCAT) 1, which is the most important isozyme for DPPC synthesis among the four LPCAT isozymes [29], did not differ between WT and KO mice (Suppl. Fig. 3A). In addition, ACSL4 deficiency did not induce the expression of other ACSL isozymes (ACSL1, 3, 5, and 6) (Suppl. Fig. 3B). Although further studies are needed to clarify how ACSL4 deficiency reduced DPPC levels in lung, these results indicated that ACSL4 plays a critical role in the remodeling of the majority of PUFA-containing glycerophospholipids in lung.

3.2. Effect of ACSL4 deficiency on PQ-induced lung injury

We next evaluated whether the alteration of phospholipid composition in lung due to ACSL4 deficiency affected sensitivity to PQ, a highly toxic compound known to induce lung damage and death. We compared the effects of a low dose (25 mg/kg body weight) of PQ administered by intraperitoneal injection in WT and ACSL4 KO mice. As shown in Fig. 2A, PQ-administered WT mice tended to have the most deaths per day on days 3–4; and most deaths occurred by day 7 after administration. Only 20% of WT mice had survived by day 28 after administration. On the other hand, ACSL4 KO mice were extremely resistant to PQ; 66.7% of KO mice had survived at 28 days after administration.

To assess the degree of PQ-induced acute lung lesions, we next performed histological analysis of lungs on day 3 after administration. Our micro-CT analysis showed no difference in histological images between the lungs of nontreated WT and KO mice (Fig. 2B). The predicted lung volume per body weight was also not different between nontreated WT and KO mice (Fig. 2C). In the lung of WT mice on day 3 after administration of PQ, x-ray transparency was remarkably decreased (Fig. 2B). This indicated a large accumulation of exudates into lung tissues. Similar changes in histological images were also observed in ACSL4 KO mice, but the degree of lesions was significantly lower in KO mice. The predicted lung volume was not affected by PQ administration in KO mice (Fig. 2C). These results indicated that PQ treatment inhibits normal gas exchange, resulting in lethal lung injury in WT mice, whereas lung impairment is less severe in KO mice. Furthermore, our HE staining analysis also showed that ACSL4 deficiency attenuated PQ-induced lung injury. As shown in Fig. 2D, hypertrophy of alveolar cells was observed in PQ-administered WT mice but not in KO mice. These results confirmed that ACSL4 deficiency significantly reduced the acute lung toxicity of PQ.

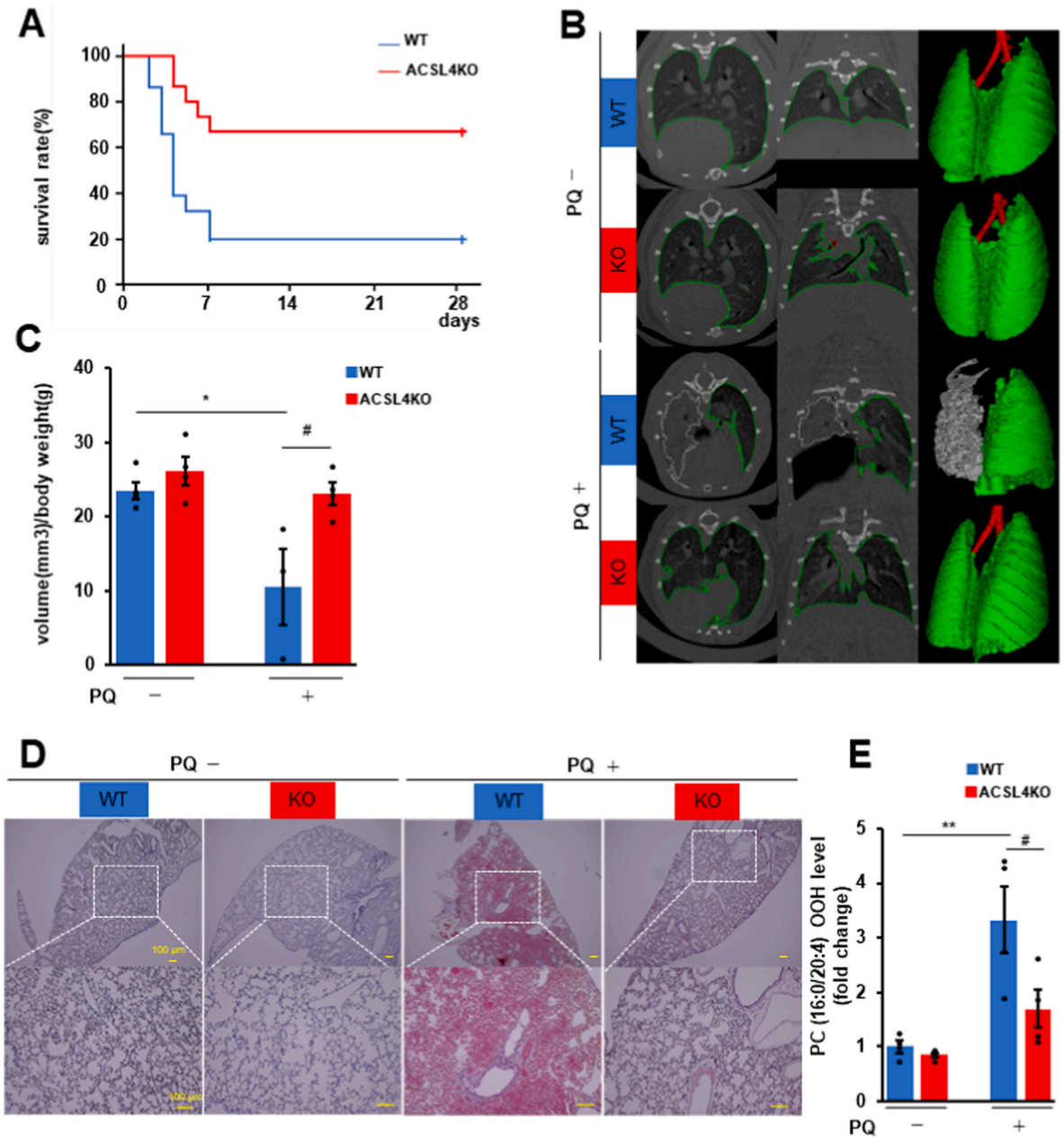

Fig. 2. Effects of ACSL4 deficiency on PQ-induced lung injury. (A) Survival curves of PQ-administered WT (blue line) and ACSL4 KO mice (red line) for 28 days; n = 15/group, generalized Wilcoxon test. **(B)** Representative micro-CT 2D images (left) and 3D image segmentation (right) of lung tissues of untreated and PQ-administered WT and ACSL4 KO mice. In 3D image segmentation, lung field area and airway are shown in green and red, respectively. The regions that are not clearly detectable due to severe damage are shown in gray. **(C)** The predicted lung volume per body weight of untreated or PQ-administered WT (blue columns) and ACSL4-KO mice (red columns); n = 3–5/group. **(D)** Representative histological images of lung tissue of untreated or PQ-administered WT and ACSL4-KO mice with HE staining. The scale bars represent 100 μm. **(E)** The level of PC 16:0/20:4-OOH in lung tissues of untreated or PQ-administered WT (blue columns) and ACSL4-KO mice (red columns); n = 4/group. Data represent means ± SEM. $*p < 0.05$ and $**p < 0.01$, untreated WT vs PQ-administered WT mice; $\#p < 0.05$ and $\#\#p < 0.01$, PQ-administered WT vs ACSL4 KO mice. (For interpretation of the references to color in this figure legend, the reader is referred to the Web version of this article.)

Since PQ is known to generate ROS, which in turn induce lipid peroxidation leading to cell death in lung tissues, we next analyzed the level of phospholipid hydroperoxide in lung by LC-MS/MS [30]. As shown in Fig. 2E, the level of PC hydroperoxide, PC(16:0/20:4)-OOH, was significantly increased in the lungs of WT mice by PQ administration, but no increase was observed in KO mice. These results suggested that phospholipid hydroperoxides produced by oxidation of PUFA might be responsible for PQ-induced acute lung injury. Additionally, we investigated the impact of Fer-1, an inhibitor of ferroptosis [31], a regulated form of cell death associated with the buildup of lipid peroxides, on PQ-induced lung injury. However, in our experimental protocol, pretreatment with Fer-1 did not show any significant effect on PQ-induced mortality. Even when WT mice were pretreated with Fer-1, only 20% of them had survived at day 28 after PQ administration. Our histological analysis also revealed that PQ-induced lung injury was not affected by pretreatment with Fer-1 (Suppl. Fig. 2).

3.3. *Effect of ACSL4 deficiency on PQ-induced inflammation- and ferroptosis-related gene expression in lung*

We conducted RT-qPCR analysis to further investigate the effects of ACSL4 deficiency on gene expression associated with inflammation and

ferroptosis. As shown in Fig. 3A, in lung tissue on day 3 after PQ administration, the gene expression levels of inflammatory cytokines such as IL-6 and IL-1β were elevated, but ACSL4 gene deletion suppressed these increments. Furthermore, the expression of cyclooxygenase 2 (COX-2), which is involved in the arachidonic acid cascade and associated with inflammation and ferroptosis [25,32], was increased in lung tissues of PQ-administered WT mice, while its upregulation was suppressed in ACSL4 KO mice.

We further found that PQ administration downregulated GPx4 expression but conversely ACSL4 was upregulated in lung. GPx4 converts phospholipid hydroperoxide to phospholipid hydroxide and suppresses the onset of ferroptosis, and both the deletion and inhibition of GPx4 are known to promote ferroptosis. As shown in Fig. 3A, the expression level of GPx4 was decreased in lung tissues of WT mice by PQ administration, but its expression was not affected in ACSL4 KO mice. On the other hand, the expression level of ACSL4 was upregulated in lung tissue, particularly in the airway epithelial cells, by PQ administration (Suppl. Fig. 3). These results suggested that the downregulation of GPx4 and the upregulation of ACSL4 might cooperatively accelerate PQ-induced lipid peroxidation.

Previous studies reported that migration of neutrophils exacerbates PQ-induced acute lung injury and spreads inflammation leading to respiratory failure. Therefore, we investigated the impact of ACSL4 deficiency on the expression of chemokines and the migration of leukocytes into lung tissues in response to PQ administration. Our RT-qPCR analysis revealed that mRNA levels of chemokines, including CXCL1, CXCL2, and CXCL5, as well as the expression of the chemokine receptor CXCR2, were upregulated in WT mice on day 3 after PQ administration. However, these increases were significantly suppressed in ACSL4 KO mice (Fig. 3A). Moreover, our immunohistochemical analysis showed that Gr-1-positive neutrophils migrated into lung tissues by PQ administration (Fig. 3B). Flow cytometry analysis also revealed an increase in $CD11b^{+}Ly6G/6C^{+}$ neutrophils in the BALF of PQ-treated WT mice (Fig. 3C). In ACSL4 KO mice, the migration of neutrophils was found to be significantly suppressed compared to WT mice in response to PQ administration. Additionally, while the migration of $CD11b^{+}F4/80^{+}$ macrophages was increased in PQ-treated WT mice, this migration was also suppressed in ACSL4 KO mice, although to a lesser extent compared to the migration of neutrophils. These results indicated that ACSL4 deficiency suppressed the migration of leukocytes, especially neutrophils, which are considered to lead to PQ-induced acute lung injury. PQ-induced lipid peroxidation might trigger the migration of neutrophils and macrophages into lung tissues.

3.4. *Effect of ACSL4 deficiency on MTX-induced side effects such as pulmonary fibrosis*

Furthermore, we investigated the effects of ACSL4 deficiency on MTX-induced pulmonary fibrosis. The treatment of MTX in our protocol did not cause WT mice to die but did induce pulmonary fibrosis. As shown in Fig. 4A, pathological damage to lung, such as alveolar wall thickening, was observed in MTX-administered WT mice. On the other hand, MTX-induced alveolar wall thickening was alleviated in ACSL4 KO mice. The content of hydroxyproline, a fibrosis biomarker [26], of whole lung also increased by treatment with MTX in WT mice, but the increase in hydroxyproline content was suppressed by ACSL4 deficiency (Fig. 4B).

We further investigated the effects of ACSL4 deficiency on the level of phospholipid hydroperoxide and the expression levels of inflammation- and ferroptosis-related genes in the lungs of MTX-treated mice. As shown in Fig. 4C, the level of PC(16:0/20:4)-OOH was reduced in ACSL4 KO mice. The expression of IL-1β, IL-6, and COX-2 genes tended to be upregulated by MTX administration, but ACSL4 deficiency did not significantly affect expression levels (Suppl. Fig. 4). Although downregulation of GPx4 expression was not observed in MTX-treated mice, the expression of ACSL4 was upregulated in the lung tissue by MTX administration. As the expressions of COX-2 and ACSL4 are reported to be induced in ferroptosis, we next examined the effect of Fer-1 on MTX-induced pulmonary fibrosis. We found that pretreatment with Fer-1 significantly suppressed the MTX-induced increase in the hydroxyproline content of lung tissues (Fig. 4D). These results suggested that ACSL4 deficiency might attenuate the lung toxicity of MTX by suppressing lipid peroxidation-mediated ferroptosis.

4. Discussion

In this study, we revealed that ACSL4 deficiency reduced the levels of PUFA-containing membrane phospholipid in mouse lung tissues (Fig. 1) and then attenuated both PQ- and MTX-induced pulmonary toxicity. In addition to ACSL isozymes, several enzymes, such as phospholipase A_2 and LPCAT, are involved in membrane phospholipid remodeling [29,33,34]. All five ACSL isozymes (ACSL-1, 3, 4, 5, and 6), are expressed in lung tissues, but our findings indicated that, among these enzymes, ACSL4 might be critical for the maintenance of membrane phospholipid composition. It is noteworthy that the DPPC level in lung tissues was also significantly reduced in ACSL4 KO mice compared to WT mice. We previously reported that the DPPC level in BMDMs was also decreased by ACSL4 deficiency [18]. Although further studies are needed to clarify the mechanism by which the DPPC level is regulated, there might be some kind of sensing and regulatory machinery that maintains the membrane's physicochemical properties. In ACSL4 KO mice, this machinery might detect a reduction in PUFA-containing.

We found that ACSL4 deficiency decreased both PQ-induced mortality and lung inflammatory reactions (Figs. 2 and 3). PQ radical, which is generated from PQ in lung tissues, donates an electron to oxygen, leading to the formation of superoxide anion, which can act as an electron donor in the generation of hydroxyl radical [5]. Since the reduction in PUFA-containing phospholipids resulted in the attenuation of PQ-induced lung lesions, PUFA-containing membrane phospholipids might be critical targets for PQ-derived hydroxyl radicals. Lipid peroxides produced by the action of PQ-derived hydroxyl radicals might not only directly damage cellular membranes of lung tissue cells but also trigger the migration of neutrophils into lung tissues to induce inflammatory reactions, thus causing mice to die. It has been reported that ferroptotic cells, which die by lipid peroxides, can promote the migration of macrophages and neutrophils towards inflamed sites through the process of chemotaxis [35,36]. Even in lung tissues of PQ-administered mice, cells that were killed by PQ-derived hydroxyl radicals might induce the chemotaxis of neutrophils and then exacerbate lung inflammation, leading to somatic death.

The lung tissues of PQ-treated WT mice showed the accumulation of lipid peroxides and the downregulation of GPx4 expression (Figs. 2 and 3). Furthermore, in addition to the upregulation of inflammation-related gene expressions, the expressions of COX-2 and ACSL4, both known to be induced in ferroptosis [21,25], were also found to be upregulated. These findings indicated that ferroptosis is likely involved in PQ-induced lung injury. It has been reported that alveolar epithelial cells are specific targets of PQ toxicity [37]. Our histological analysis further revealed that ACSL4 protein is expressed and upregulated in alveolar epithelial cells (Suppl. Fig. 2D). Ferroptosis of alveolar epithelial cells might be critical for PQ-induced lung injury. We therefore attempted to examine the effects of Fer-1, an inhibitor of ferroptosis [31], but we found that it did not improve PQ-induced mortality. Lung damage by PQ administration might be too massive for the preventive effects of Fer-1.

ACSL4 deficiency was found to attenuate MTX-induced lung fibrosis (Fig. 4). MTX inhibits dihydrofolate reductase, which reduces folic acid to tetrahydrofolic acid and catalyzes the regeneration of tetrahydrobiopterin [38]. Since tetrahydrobiopterin is a potent radical-trapping antioxidant [39,40], it has been suggested that MTX might upregulate ROS generation by decreasing in tetrahydrobiopterin levels. The increase in ROS levels by MTX administration might be involved in MTX-induced pulmonary toxicity, but the precise mechanism by which

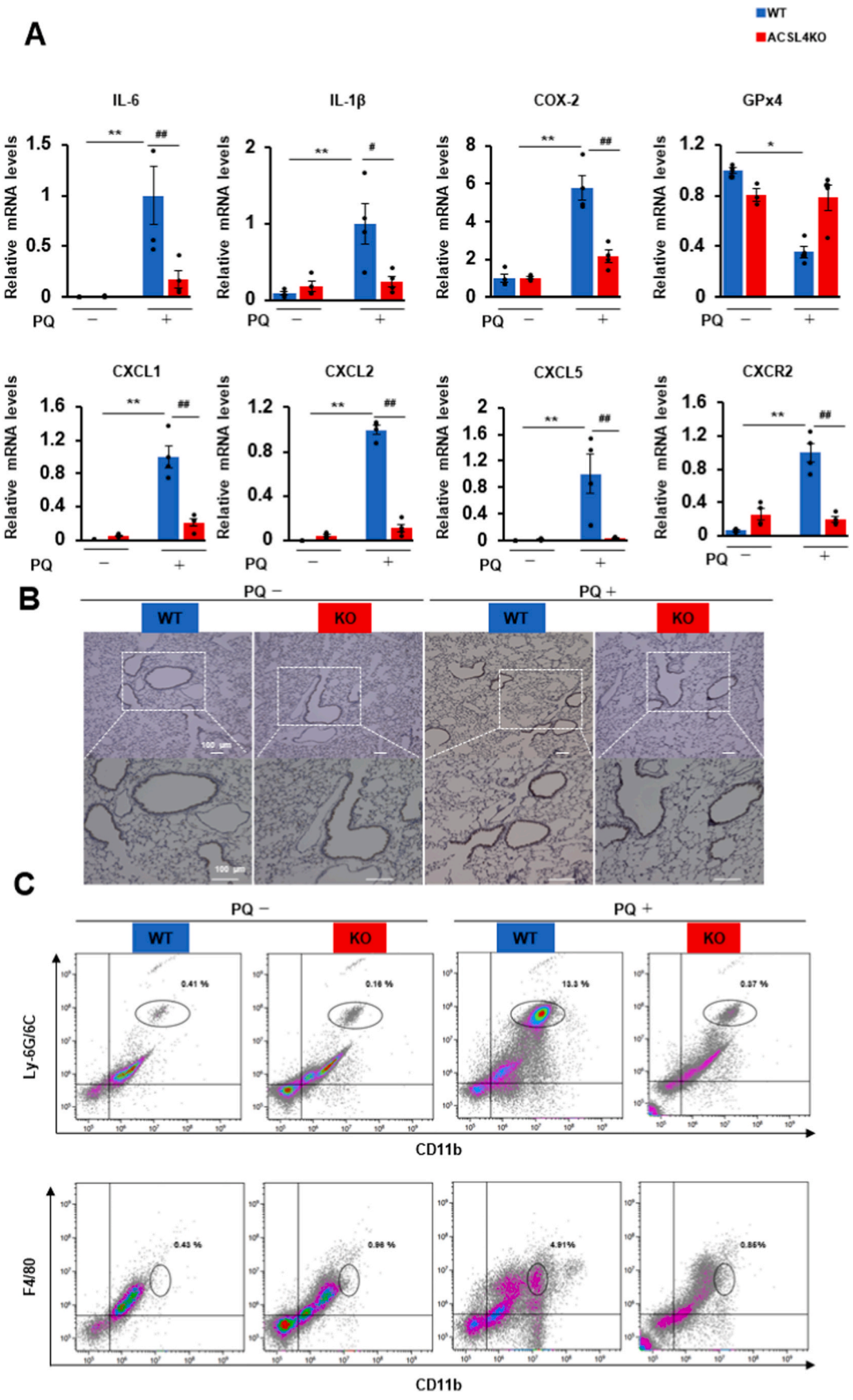

(caption on next page)

Fig. 3. Effects of ACSL4 deficiency on PQ-induced lung inflammation. (A) mRNA expression levels of inflammatory cytokines (IL-6 and IL-1β), COX-2, GPx4, and chemokines (CXCL1, CXCL2, CXCL5, and CXCR2) in lung tissues of untreated or PQ-administered WT (blue columns) and ACSL4-KO mice (red columns); n = 4/group. $*p < 0.05$ and $**p < 0.01$, untreated WT vs PQ-administered WT mice; $\#p < 0.05$ and $\#\#p < 0.01$, PQ-administered WT vs ACSL4 KO mice. **(B)** Representative Gr-1 staining images of lung tissue of untreated or PQ-administered WT and ACSL4-KO mice. The scale bars represent 100 μm. **(C)** Flow cytometry analysis of $CD11b^{+}Ly6G/6C^{+}$ neutrophils (upper) and $CD11^{+}F4/80+$ macrophages (lower) in the BAL fluid cells of untreated or PQ-administered WT and ACSL4-KO mice; cell samples were pooled from 5 mice per group. (For interpretation of the references to color in this figure legend, the reader is referred to the Web version of this article.)

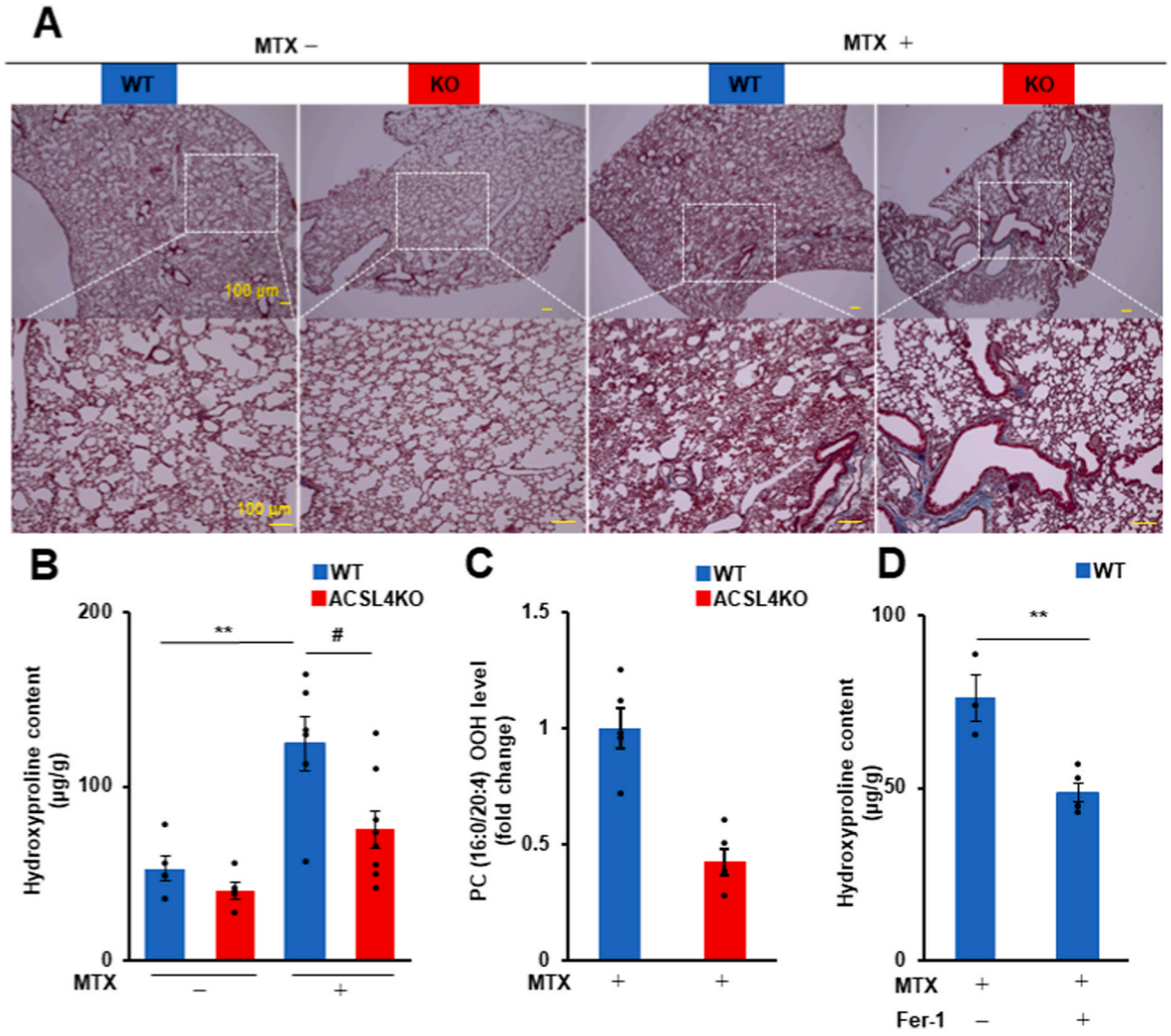

Fig. 4. Effects of ACSL4 deficiency on MTX-induced lung fibrosis. (A) Representative histological images of lung tissues of untreated or MTX-treated WT and ACSL4-KO mice stained with Masson's trichrome staining. **(B)** Hydroxyproline levels in lung tissues of untreated or MTX-treated WT (blue columns) and ACSL4-KO mice (red columns). n = 5–8/group. $*p < 0.05$ and $**p < 0.01$, untreated WT vs MTX-administered WT mice; $\#p < 0.05$, MTX-administered WT vs ACSL4 KO mice. **(C)** The level of PC 16:0/20:4-OOH in lung tissues of MTX-administered WT (blue columns) and ACSL4-KO mice (red columns); n = 5/group. Data represent means ± SEM. $\#\#p < 0.01$, MTX-administered WT vs ACSL4 KO mice. **(D)** Hydroxyproline levels in lung tissues of Fer-1-pretreated MTX-treated WT mice. n = 3/group. $**p < 0.01$, unpretreated vs Fer-1-pretreated WT mice. (For interpretation of the references to color in this figure legend, the reader is referred to the Web version of this article.)

MTX induces lung fibrosis remains unclear. We here found that the level of phospholipid hydroperoxide was reduced in the lungs of MTX-administered ACSL4 KO mice. The expression levels of ferroptosis-related genes, COX-2 and ACSL4, were upregulated by MTX administration. Notably, both ACSL4 deficiency and pretreatment with Fer-1, a ferroptosis inhibitor, were found to suppress MTX-induced lung fibrosis (Fig. 4). Our findings indicated that, similar to PQ, MTX might prompt peroxidation of PUFA-containing phospholipids in lung tissues and then induce lung fibrosis through ferroptosis. It is well known that long-term use of MTX often results in pulmonary fibrosis as an adverse side effect [7–9]. ACSL4 inhibitors and ferroptosis inhibitors may be potential targets for reducing the adverse side effects of MTX.

In conclusion, we here showed that ACSL4 gene deletion down-regulates various kinds of phospholipid species containing PUFA in the mouse lung, and then mitigates pulmonary toxic chemical-induced lung injury by suppressing lipid peroxidation. Inhibition of ACSL4 may be promising for the prevention and treatment of chemical-induced lung injury.

Funding

This work was supported in part by Grants-in Aid for Scientific Research (B) (16H05108 and 19H03375) (S.H.) and for Scientific Research (C) (19K07087) (H.K.) from the Japan Society for the

Promotion of Science and by a grant for a Private University High Technology Research Center Project from the Ministry of Education, Culture, Sports, Science, Culture, and Technology of Japan.

Declaration of competing interest

The authors declare no conflicts of interest associated with this manuscript.

Data availability

Data will be made available on request.

Acknowledgments

We thank the members of Division of Health Chemistry for their helpful discussions and comments, and are grateful to Dr. T. Sakamoto and Professor K. Imai (Kitasato University) for conducting the LC-MS/MS analysis of phospholipid hydroperoxides.

Appendix A. Supplementary data

Supplementary data to this article can be found online at https://doi.org/10.1016/j.redox.2023.102850.

References

[1] H.K. Fisher, J.A. Clements, R.R. Wright, Enhancement of oxygen toxicity by the herbicide paraquat, Am. J. Respir. Crit. Care Med. 107 (1973) 246–252, https://doi.org/10.1164/arrd.1973.107.2.246.

[2] D.C. Phillips, K.J. Woollard, H.R. Griffiths, The anti-inflammatory actions of methotrexate are critically dependent upon the production of reactive oxygen species, Br. J. Pharmacol. 138 (2003) 501–511, https://doi.org/10.1038/sj.bjp.0705054.

[3] S.J. Seok, H.W. Gil, D.S. Jeong, J.O. Yang, E.Y. Lee, S.Y. Hong, Paraquat intoxication in subjects who attempt suicide: why they chose paraquat, Korean. J. Intern. Med. 24 (2009) 247–251, https://doi.org/10.3904/kjim.2009.24.3.247.

[4] P.H. Hoet, C.P. Lewis, M. Demedts, B. Nemery, Putrescine and paraquat uptake in human lung slices and isolated type II pneumocytes, Biochem. Pharmacol. 48 (1994) 517–524, https://doi.org/10.1016/0006-2952(94)90281-x.

[5] T. Blanco-Ayala, A.C. Andérica-Romero, J. Pedraza-Chaverri, New insights into antioxidant strategies against paraquat toxicity, Free Radic. Res. 48 (2014) 623–640, https://doi.org/10.3109/10715762.2014.899694.

[6] M. Cutolo, A. Sulli, C. Pizzorni, B. Seriolo, R.H. Straub, Anti-inflammatory mechanisms of methotrexate in rheumatoid arthritis, Ann. Rheum. Dis. 60 (2001) 729–735, https://doi.org/10.1136/ard.60.8.729.

[7] R.J. McKendry, P. Dale, Adverse effects of low dose methotrexate therapy in rheumatoid arthritis, J. Rheumatol. 20 (1993) 1850–1856.

[8] P. Emery, F.C. Breedveld, S. Hall, P. Durez, D.J. Chang, D. Robertson, A. Singh, R. D. Pedersen, A.S. Koenig, B. Freundlich, Comparison of methotrexate monotherapy with a combination of methotrexate and etanercept in active, early, moderate to severe rheumatoid arthritis (COMET): a randomised, double-blind, parallel treatment trial, Lancet 372 (2008) 375–382, https://doi.org/10.1016/s0140-6736(08)61000-4.

[9] J.M. Kremer, G.S. Alarcón, M.E. Weinblatt, M.V. Kaymakcian, M. Macaluso, G. W. Cannon, W.R. Palmer, J.S. Sundy, E.W. St Clair, R.W. Alexander, G.J. Smith, C. A. Axiotis, Clinical, laboratory, radiographic, and histopathologic features of methotrexate-associated lung injury in patients with rheumatoid arthritis: a multicenter study with literature review, Arthritis Rheumatol. 40 (1997) 1829–1837, https://doi.org/10.1002/art.1780401016.

[10] S. Herman, N. Zurgil, M. Deutsch, Low dose methotrexate induces apoptosis with reactive oxygen species involvement in T lymphocytic cell lines to a greater extent than in monocytic lines, Inflamm. Res. 54 (2005) 273–280, https://doi.org/10.1007/s00011-005-1355-8.

[11] R. Mammadov, B. Suleyman, S. Akturan, F.K. Cimen, N. Kurt, Z. Suleyman, İ. Malkoc, Effect of lutein on methotrexate-induced oxidative lung damage in rats: a biochemical and histopathological assessment, Korean J. Intern. Med. 34 (2019) 1279–1286, https://doi.org/10.3904/kjim.2018.145.

[12] S. Dalleau, M. Baradat, F. Guéraud, L. Huc, Cell death and diseases related to oxidative stress: 4-hydroxynonenal (HNE) in the balance, Cell Death Differ. 20 (2013) 1615–1630, https://doi.org/10.1038/cdd.2013.138.

[13] G.P. Voulgaridou, I. Anestopoulos, R. Franco, M.I. Panayiotidis, A. Pappa, DNA damage induced by endogenous aldehydes: current state of knowledge, Mutat. Res. 711 (2011) 13–27, https://doi.org/10.1016/j.mrfmmm.2011.03.006.

[14] D.G. Mashek, K.E. Bornfeldt, R.A. Coleman, J. Berger, D.A. Bernlohr, P. Black, C. C. DiRusso, S.A. Farber, W. Guo, N. Hashimoto, V. Khodiyar, F.A. Kuypers, L. J. Maltais, D.W. Nebert, A. Renieri, J.E. Schaffer, A. Stahl, P.A. Watkins, V. Vasiliou, T.T. Yamamoto, Revised nomenclature for the mammalian long-chain acyl-CoA synthetase gene family, J. Lipid Res. 45 (2004) 1958–1961, https://doi.org/10.1016/j.mrfmmm.2011.03.006.

[15] M.J. Kang, T. Fujino, H. Sasano, H. Minekura, N. Yabuki, H. Nagura, H. Iijima, T. T. Yamamoto, A novel arachidonate-preferring acyl-CoA synthetase is present in steroidogenic cells of the rat adrenal, ovary, and testis, Proc. Natl. Acad. Sci. U.S.A. 94 (1997) 2880–2884, https://doi.org/10.1073/pnas.94.7.2880.

[16] H. Kuwata, M. Yoshimura, Y. Sasaki, E. Yoda, Y. Nakatani, I. Kudo, S. Hara, Role of long-chain acyl-coenzyme A synthetases in the regulation of arachidonic acid metabolism in interleukin 1β-stimulated rat fibroblasts, Biochim. Biophys. Acta 1841 (2014) 44–53, https://doi.org/10.1016/j.bbalip.2013.09.015.

[17] E.A. Killion, A.R. Reeves, M.A. El Azzouny, Q.W. Yan, D. Surujon, J.D. Griffin, T. A. Bowman, C. Wang, N.R. Matthan, E.L. Klett, D. Kong, J.W. Newman, X. Han, M. J. Lee, R.A. Coleman, A.S. Greenberg, A role for long-chain acyl-CoA synthetase-4 (ACSL4) in diet-induced phospholipid remodeling and obesity-associated adipocyte dysfunction, Mol. Metabol. 9 (2018) 43–56, https://doi.org/10.1016/j.molmet.2018.01.012.

[18] H. Kuwata, E. Nakatani, S. Shimbara-Matsubayashi, F. Ishikawa, M. Shibanuma, Y. Sasaki, E. Yoda, Y. Nakatani, S. Hara, Long-chain acyl-CoA synthetase 4 participates in the formation of highly unsaturated fatty acid-containing phospholipids in murine macrophages, Biochim. Biophys. Acta 1864 (2019) 1606–1618, https://doi.org/10.1016/j.bbalip.2019.07.013.

[19] S.J. Dixon, K.M. Lemberg, M.R. Lamprecht, R. Skouta, E.M. Zaitsev, C.E. Gleason, D.N. Patel, A.J. Bauer, A.M. Cantley, W.S. Yang, B. Morrison 3rd, B.R. Stockwell, Ferroptosis: an iron-dependent form of nonapoptotic cell death, Cell 149 (2012) 1060–1072, https://doi.org/10.1016/j.cell.2012.03.042.

[20] B.R. Stockwell, J.P. Friedmann Angeli, H. Bayir, A.I. Bush, M. Conrad, S.J. Dixon, S. Fulda, S. Gascón, S.K. Hatzios, V.E. Kagan, K. Noel, X. Jiang, A. Linkermann, M. E. Murphy, M. Overholtzer, A. Oyagi, G.C. Pagnussat, J. Park, Q. Ran, C. S. Rosenfeld, K. Salnikow, D. Tang, F.M. Torti, S.V. Torti, S. Toyokuni, K. A. Woerpel, D.D. Zhang, Ferroptosis: a regulated cell death nexus linking metabolism, redox biology, and disease, Cell 171 (2017) 273–285, https://doi.org/10.1016/j.cell.2017.09.021.

[21] S. Doll, B. Proneth, Y.Y. Tyurina, E. Panzilius, S. Kobayashi, I. Ingold, M. Irmler, J. Beckers, M. Aichler, A. Walch, H. Prokisch, D. Trümbach, G. Mao, F. Qu, H. Bayir, J. Füllekrug, C.H. Scheel, W. Wurst, J.A. Schick, V.E. Kagan, J.P. Angeli, M. Conrad, ACSL4 dictates ferroptosis sensitivity by shaping cellular lipid composition, Nat. Chem. Biol. 13 (2017) 91–98, https://doi.org/10.1038/nchembio.2239.

[22] V.E. Kagan, G. Mao, F. Qu, J.P. Angeli, S. Doll, C.S. Croix, H.H. Dar, B. Liu, V. A. Tyurin, V.B. Ritov, A.A. Kapralov, A.A. Amoscato, J. Jiang, T. Anthonymuthu, D. Mohammadyani, Q. Yang, B. Proneth, J. Klein-Seetharaman, S. Watkins, I. Bahar, J. Greenberger, R.K. Mallampalli, B.R. Stockwell, Y.Y. Tyurina, M. Conrad, H. Bayır, Oxidized arachidonic and adrenic PEs navigate cells to ferroptosis, Nat. Chem. Biol. 13 (2017) 81–90, https://doi.org/10.1038/nchembio.2238.

[23] H. Yuan, X. Li, X. Zhang, R. Kang, D. Tang, Identification of ACSL4 as a biomarker and contributor of ferroptosis, Biochem. Biophys. Res. Commun. 478 (2016) 1338–1343, https://doi.org/10.1016/j.bbrc.2016.08.124.

[24] W.S. Yang, R. SriRamaratnam, M.E. Welsch, K. Shimada, R. Skouta, V. S. Viswanathan, J.H. Cheah, P.A. Clemons, A.F. Shamji, C.B. Clish, L.M. Brown, A. W. Girotti, V.W. Cornish, S.L. Schreiber, B.R. Stockwell, Regulation of ferroptotic cancer cell death by GPX4, Cell 156 (2014) 317–331, https://doi.org/10.1016/j.cell.2013.12.010.

[25] N. Yamada, T. Karasawa, H. Kimura, S. Watanabe, T. Komada, R. Kamata, A. Sampilvanjil, J. Ito, K. Nakagawa, H. Kuwata, S. Hara, K. Mizuta, Y. Sakuma, N. Sata, M. Takahashi, Ferroptosis driven by radical oxidation of n-6 polyunsaturated fatty acids mediates acetaminophen-induced acute liver failure, Cell Death Dis. 11 (2020) 144, https://doi.org/10.1038/s41419-020-2334-2.

[26] M. Ohbayashi, S. Kubota, A. Kawase, N. Kohyama, Y. Kobayashi, T. Yamamoto, Involvement of epithelial-mesenchymal transition in methotrexate-induced pulmonary fibrosis, J. Toxicol. Sci. 39 (2014) 319–330, https://doi.org/10.2131/jts.39.319.

[27] E.S. Brown, Isolation and assay of dipalmityl lechitin in lung extracts, Am. J. Physiol. 207 (1964) 402–406, https://doi.org/10.1152/ajplegacy.1964.207.2.402.

[28] T.E. Morgan, T.N. Finley, H. Fialkow, Comparison of the composition and surface activity of "alveolar" and whole lung lipids in the dog, Biochim. Biophys. Acta 106 (1965) 403–413, https://doi.org/10.1016/0005-2760(65)90049-4.

[29] H. Nakanishi, H. Shindou, D. Hishikawa, T. Harayama, R. Ogasawara, A. Suwabe, R. Taguchi, T. Shimizu, Cloning and characterization of mouse lung-type acyl-CoA: lysophosphatidylcholine acyltransferase 1 (LPCAT1). Expression in alveolar type II cells and possible involvement in surfactant production, J. Biol. Chem. 281 (2006) 20140–20147, https://doi.org/10.1074/jbc.M600225200.

[30] T. Sakamoto, K. Maebayashi, Y. Nakagawa, H. Imai, Deletion of the four phospholipid hydroperoxide glutathione peroxidase genes accelerates aging in *Caenorhabditis elegans*, Gene Cell. 19 (2014) 778–792, https://doi.org/10.1111/gtc.12175.

[31] P. Liu, Y. Feng, H. Li, X. Chen, G. Wang, S. Xu, Y. Li, L. Zhao, Ferrostatin-1 alleviates lipopolysaccharide-induced acute lung injury via inhibiting ferroptosis, Cell. Mol. Biol. Lett. 25 (2020) 10, https://doi.org/10.1186/s11658-020-00205-0.

[32] X.Y. Mao, H.H. Zhou, W.L. Jin, Ferroptosis induction in pentylenetetrazole kindling and pilocarpine-induced epileptic seizures in mice, Front. Neurosci. 13 (2019) 721, https://doi.org/10.3389/fnins.2019.00721.

[33] T. Shimizu, Lipid mediators in health and disease: enzymes and receptors as therapeutic targets for the regulation of immunity and inflammation, Annu. Rev. Pharmacol. Toxicol. 49 (2009) 123–150, https://doi.org/10.1146/annurev.pharmtox.011008.145616.

[34] S. Hara, E. Yoda, Y. Sasaki, Y. Nakatani, H. Kuwata, Calcium-independent phospholipase $A_2\gamma$ ($iPLA_2\gamma$) and its roles in cellular functions and diseases, Biochim. Biophys. Acta 1864 (2019) 861–868, https://doi.org/10.1016/j.bbalip.2018.10.009.

[35] Y. Wang, F. Quan, Q. Cao, Y. Lin, C. Yue, R. Bi, X. Cui, H. Yang, Y. Yang, L. Birnbaumer, X. Li, X. Gao, Quercetin alleviates acute kidney injury by inhibiting ferroptosis, J. Adv. Res. 28 (2021) 231–243, https://doi.org/10.1016/j.redox.2022.102262.

[36] Y. Wang, M. Zhang, R. Bi, Y. Su, F. Quan, Y. Lin, C. Yue, X. Cui, Q. Zhao, S. Liu, Y. Yang, D. Zhang, Q. Cao, X. Gao, ACSL4 deficiency confers protection against ferroptosis-mediated acute kidney injury, Redox Biol. 51 (2022), 102262, https://doi.org/10.1016/j.redox.2022.102262.

[37] L.L. Smith, Paraquat toxicity, Philos. Trans. R. Soc. Lond. B Biol. Sci. 311 (1985) 647–657, https://doi.org/10.1098/rstb.1985.0170.

[38] M. Soula, R.A. Weber, O. Zilka, H. Alwaseem, K. La, F. Yen, H. Molina, J. Garcia-Bermudez, D.A. Pratt, K. Birsoy, Metabolic determinants of cancer cell sensitivity to canonical ferroptosis inducers, Nat. Chem. Biol. 16 (2020) 1351–1360, https://doi.org/10.1016/j.redox.2022.102262.

[39] S. Kojima, S. Ona, I. Iizuka, T. Arai, H. Mori, K. Kubota, Antioxidative activity of 5,6,7,8-tetrahydrobiopterin and its inhibitory effect on paraquat-induced cell toxicity in cultured rat hepatocytes, Free Radic. Res. 23 (1995) 419–430, https://doi.org/10.3109/10715769509065263.

[40] R.S. Shen, Inhibition of dopamine autoxidation by tetrahydrobiopterin and NADH in the presence of dihydropteridine reductase, Neurotoxicology 12 (1991) 201–208.